

17 **Abstract**

18 Environmental impacts resulting from historic lead and zinc mining in Kabwe, Zambia affect
19 human health due to the dust generated from the mine waste that contains lead, a known
20 hazardous pollutant. We employed microbially induced calcium carbonate precipitation (MICP),
21 an alternative capping method, to prevent dust generation and reduce the mobility of
22 contaminants. Pb-resistant *Oceanobacillus profundus* KBZ 1-3 and *O. profundus* KBZ 2-5
23 isolated from Kabwe were used to biocement the sand that would act as a cover to prevent dust
24 and water infiltration. Sand biocemented by KBZ 1-3 and KBZ 2-5 had maximum unconfined
25 compressive strength values of 3.2 MPa and 5.5 MPa, respectively. Additionally, biocemented
26 sand exhibited reduced water permeability values of 9.6×10^{-8} m/s and 8.9×10^{-8} m/s for *O.*
27 *profundus* KBZ 1-3 and KBZ 2-5, respectively, which could potentially limit the entrance of
28 water and oxygen into the dump, hence reducing the leaching of heavy metals. We propose that
29 these isolates represent an option for bioremediating contaminated waste by preventing both
30 metallic dust from becoming airborne and rainwater from infiltrating into the waste. *O. profundus*
31 KBZ 1-3 and *O. profundus* KBZ 2-5 isolated from Kabwe represent a novel species that has, for
32 the first time, been applied in a bioremediation study.

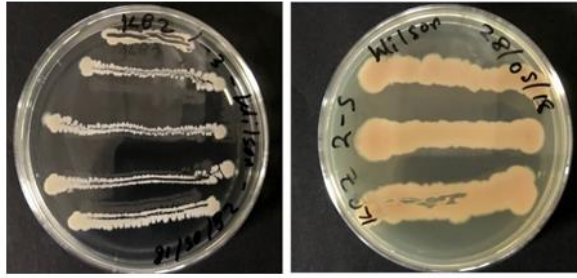
33

34 **Highlights**

- 35 • Mine waste dump causing chronic Pb poisoning to humans by inhaling airborne dust
- 36 • Proposed to use biomineralization to prevent the generation of dust
- 37 • Isolated indigenous biomineralization bacteria showing biocementation capability
- 38 • Capping mine waste by biomineralizing bacteria that reduce risk to human health
- 39 • Effective, sustainable and novel approach to eliminate Pb poisoning

40

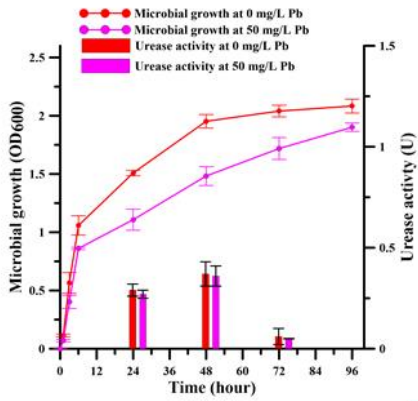
Bacteria isolated from Pb-contaminated site



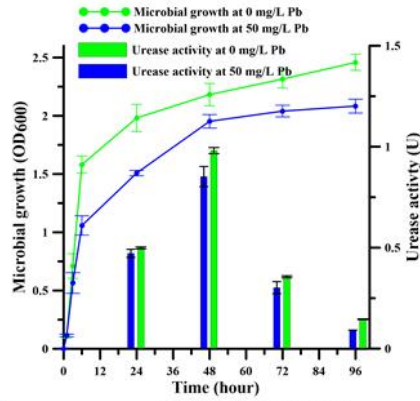
KBZ 1-3

KBZ 2-5

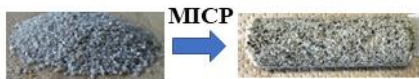
Microbial growth and urease activity in Pb (II)



O. profundus KBZ 1-3



O. profundus KBZ 2-5



MICP



MICP

42 **1 Introduction**

43 Kabwe Mine was a lead and zinc mine that commenced its operations in 1902 until its closure
44 in 1994. Apart from lead and zinc, it also produced silver, manganese, cadmium, vanadium, and
45 titanium in smaller quantities (Mufinda, 2015). Due to the extraction of different minerals, several
46 mineral processing techniques were used resulting in the production of, different types of mine
47 waste dumps (Fig. 1a). Several studies have cited chronic Pb poisoning in humans, and
48 contamination of soil, water, and sediments in the mine and the surrounding areas (Kribek et al.,
49 2009; Tembo et al., 2006; Yabe et al., 2015; Yabe et al., 2018). The current blood levels of Pb in
50 children exceeds 45 $\mu\text{g/dL}$, much higher than the recommended level of 5 $\mu\text{g/dL}$ (Kosnett et al.,
51 2007; Yabe et al., 2015). The predominant reason for this high Pb level in blood is the airborne
52 Pb metallic dusts emanating from the mine waste dump. These dusts are blown by the prevailing
53 winds into the residential areas, and due to their fine particulate nature, are either inhaled or
54 ingested (Yabe et al., 2015). Leach plant residues and kiln slag, shown in Fig. 1b, are susceptible
55 to wind and water erosion. These two types of wastes were selected for immobilization because
56 they are deemed to be the most toxic and are distributed over the largest area onsite. In response
57 to the concern of dust emanating from the mine wastes in Kabwe, remediation methods such as
58 the revegetation of the waste dump by metallophytes was proposed and implemented, but
59 subsequently failed because the plants failed to grow (Leteinturier et al., 2001). Additionally,
60 mining waste has not been re-processed due to probably the cost of metal recovery (BMR Group
61 PLC, 2019).

62 A promising technique to prevent metallic dust from becoming airborne in-situ is the
63 immobilization of these wastes by microbially induced calcium carbonate precipitation (MICP)
64 using ureolytic bacteria (Achal et al., 2013; Chen et al., 2017; Kim and Lee, 2018; Mwandira et
65 al., 2017; Nam et al., 2016; Zhu et al., 2016). MICP involves the hydrolysis of urea into
66 ammonium and carbamate by urease catalysis which results in CaCO_3 formation in the presence

67 of Ca^{2+} ions. The proposed use of MICP to cap mine wastes is expected to eliminate both dust
68 generation and water infiltration, restoring the contaminated site. Related studies have proposed
69 MICP for ground improvement (Salifu et al., 2016), coastal erosion control (Khan et al., 2015),
70 mine waste immobilization (Achal et al., 2013), self-healing concrete (Wiktor and Jonkers,
71 2011), and wastewater treatment (Torres-Aravena et al., 2018). Although many ureolytic bacteria
72 have been isolated, continued isolation and identification of more novel species, especially those
73 that are indigenous to the area, is indispensable. The present study focuses on (i) the isolation of
74 a Pb-resistant ureolytic bacteria from contaminated waste at Kabwe mine site; (ii) the
75 determination of the optimal Ca^{2+} /urea concentration, and (iii) the use of the bacteria to biocement
76 the sand. Such an investigation, involving the isolation and identification of effective
77 microorganisms for biotechnological applications, represents a sustainable approach to
78 remediation, eliminating the current environmental problems without significantly changing the
79 local ecological integrity. In this study, we introduced two new strains of ureolytic bacteria for
80 the MICP process: *Oceanobacillus profundus* KBZ 1-3 and *Oceanobacillus profundus* KBZ 2-5.

81

82 **2 Materials and methods**

83 **2.1 Soil sample collection**

84 Fig. 1a shows the locations of two soil sampling points from the abandoned Kabwe mine
85 site of Central Province, Zambia ($15^{\circ}27' - 17^{\circ}28'$ S latitude and $23^{\circ}06' - 25^{\circ}33'$ E longitude). The
86 mine waste was exported from Zambia under approval No. RCT 7686229, and the import was
87 also permitted by Plant Protection Station, Ministry of Agriculture, Forestry and Fisheries, Japan
88 under the approval No. 29-836. The samples were transported from the site to the Laboratory of
89 Biotechnology for Resource Engineering, Faculty of Engineering, Hokkaido University, Japan.

90

91 **2.2 Isolation and molecular identification of Pb-resistant bacteria**

92 Bacteria were isolated by placing 1 g of soil in a 15 mL sterile centrifuge tube and adding
93 10 mL of sterile water, followed by vigorous shaking by hand. Samples were diluted 10- to
94 10,000-fold using sterile water and plated on NH₄ YE agar medium (20 g/L yeast extract; 10 g/L
95 di-ammonium sulfate (NH₄)₂SO₄; 0.13 M tris buffer (pH = 8.0); and 20 g/L agar amended with
96 Pb(II)) to isolate Pb-resistant strains. The plates were incubated at 30 °C for 72 h. Urease activity
97 was screened according to a previous study by Danjo and Kawasaki (2015). In brief, the isolated
98 colonies were mixed with 20 mL of cresol red solution (25 g/L urea and 0.4 g/L cresol red) and
99 left standing at 45 °C for 2 h. After 2 h, the samples that changed their color to purple were
100 selected.

101 The Pb-resistant isolate was identified by 16S rRNA sequence analysis. DNA extracts were
102 amplified using two sets of primers targeting the 16S rRNA region specific for almost all bacterial
103 16S sequences: primers F9 (5'- GAGTTTGATCCTGGCTCAG -3') and R1451 (5'-
104 AAGGAGGTGATCCAGCC -3'). The PCR amplification cycle consisted of an initial
105 denaturation step of 5 min at 94 °C, followed by 25 cycles of 1 min at 94 °C, 2 min at 60 °C, and
106 1 min at 72 °C and a final extension step of 30 min at 72 °C. The amplicons were separated by
107 gel electrophoresis and the resulting DNA bands were extracted and purified using the
108 FastGene™ PCR extraction Kit following the manufacturer's instructions (Nippon Genetics Co.
109 Ltd, Tokyo, Japan). The extracted DNA was sent to Eurofins Genomics laboratory (Eurofins
110 Genomics, Tokyo, Japan) for DNA sequencing. Subsequent phylogenetic analysis was conducted
111 by TechnoSuruga Laboratory (TechnoSuruga Laboratory Company Ltd, Tokyo Japan), which
112 used the BLAST algorithm to find related sequences in the GeneBank Database, DNA Data Bank
113 of Japan and the European Molecular Biology Laboratory.

114

115 **2.3 Effect of Pb on microbial growth and urease activity of isolates**

116 Microbial growth and urease activity were measured according to the procedures reported
117 in a previous study (Mwandira et al., 2017). Microbial growth was measured by UV–vis
118 spectrophotometry (V-730, Jasco International Co., Ltd., Tokyo, Japan) that recorded optical
119 density (OD) readings at 600 nm for 96 h in the absence and presence of 50 mg/L Pb(II).
120 Experiments were conducted in triplicate.

121

122 **2.4 Determination of the optimal Ca²⁺/urea concentration**

123 Bioprecipitation experiments were carried out to determine the optimal Ca²⁺/urea
124 concentrations. The bacterial isolate was precultured for 24 h in 5 mL NH₄ YE medium, then 1
125 mL of preculture was inoculated into 100 mL of NH₄ YE medium to grow the main culture at 30
126 °C for 24 h with continuous aeration at 160 rpm. The bacterial suspension was then added to
127 different equimolar concentrations of CaCl₂ and urea (0.1 M, 0.3 M, 0.5 M, 0.75 M, and 1.0 M).
128 The mixtures were subsequently incubated for 24 h at 30 °C with shaking (160 rpm) and then
129 centrifuged (15,000 rpm for 5 min) to collect the precipitate. The precipitate was weighed and
130 then analyzed by XRD. Precipitation experiments were conducted in triplicate.

131

132 **2.5 Syringe biocementation test**

133 The Mizunami sand used in the experiments is uniformly graded with a median particle
134 size of 1.2 mm (Fig. S1). Mizunami sand was used to represent sand that can be obtained locally
135 near the contaminated site. The sand was sterilized, and hand packed into a 35-mL syringe (mean
136 diameter, D₅₀ = 2.5 cm and height, h = 7 cm), followed by the gentle injection of bacteria and
137 solidification solution as illustrated in Fig. S2 (Supplementary material). Initially bacteria
138 suspension was injected and allowed to stand in the column for 2 h and thereafter solidification
139 solution was injected. This was repeated every 24 h for a period of 14 days. Additionally, two

140 sets of biocementation experiments were conducted using conditions designed to mimic the
141 possible conditions for in-situ injection of treatment solutions. In the first set of experiments, 2
142 mL of cementation solution was left above the surface of the sand to mimic saturated conditions;
143 this procedure is called immersed method. The second set of experiments was conducted by
144 sequentially adding solution as the solution was drained; thus, this procedure is called the flow-
145 through method. Control tests were also conducted following the same procedures but without
146 the addition of bacterial cells.

147 Unconfined compressive strength (UCS) of the cemented samples was measured using a
148 needle penetration device (SH-70, Maruto Testing Machine Company, Tokyo, Japan) to
149 determine the strength of biocemented sand prepared by immersed and flow-through methods.

150 The CaCO_3 contents of the cemented samples were determined by the calcimetric method,
151 which uses 3M HCl acid and standard grade CaCO_3 (Hukue et al., 2001). In brief, 1.5 g solidified
152 sand and 15 ml HCl in plastic vials were placed in a reaction vessel which was then closed,
153 tightened, zeroed, and sealed with O-rings. The vessel was then shaken to allow HCl to react with
154 sample, producing CO_2 gas. A digital manometer measured and recorded the CO_2 gas pressure
155 readings. Same procedure was used to generate a calibration curve with known amounts of
156 CaCO_3 , which was used to quantify the readings from the specimen. The control and top center
157 part of biocemented specimens treated by immersed and flow-through methods were tested.

158

159 **2.6 Hydraulic conductivity**

160 Hydraulic conductivity was assessed by the falling head method using a DIK 4000 system
161 (Daiki Rika Kogyo Co., Ltd., Saitama, Japan). The samples were saturated with water and placed
162 in a desiccator for 48 h before the measurement of hydraulic conductivity. Hydraulic conductivity
163 was determined in control and biocemented specimens treated by both immersed and flow
164 through methods.

165 **2.7 SEM and XRD analysis**

166 The microstructure of fractions of the biocemented samples was examined by scanning
167 electron microscopy (SEM) (Miniscope TM3000, Hitachi, Tokyo, Japan). Additionally, X-ray
168 diffraction (XRD) analysis (MiniFlex™, Rigaku Co., Ltd., Tokyo, Japan) was conducted using
169 Ni-filtered Cu 1.5406 Å radiation to determine the mineral phases of both the control and
170 biocemented sand. Scans were recorded from 5° to 80° of 2θ at a rate of 20°/min.

171

172 **3 Results and discussion**

173 **3.1 Isolation of ureolytic bacteria**

174 Ureolytic bacteria were isolated based on the color change of the cresol red solution after
175 urea hydrolysis. Colonies that changed the color of the solution from yellow to purple were
176 selected. Color change is observed due to urea hydrolysis that causes the pH of the medium to
177 rise. Of the thirty-five isolates from Kabwe, only four isolates, identified as *Oceanobacillus*
178 *profundus* KBZ 1-3, *Psychrobacillus* sp. KBZ 2-2, *Oceanobacillus profundus* KBZ 2-3, and *O.*
179 *profundus* KBZ 2-5 were found to produce urease and tolerated Pb, and were screened. *O.*
180 *profundus* KBZ 1-3 and *O. profundus* KBZ 2-5 were selected for subsequent experiments because
181 they were Pb-resistant and capable of biocementation. Supplementary Fig. S3 shows the
182 neighbor-joining phylogenetic tree of *O. profundus* KBZ 1-3 and *O. profundus* KBZ 2-5, which
183 were isolated from the leach plant residue mine waste and near the wastewater pond, respectively.
184 Both *O. profundus* 1-3 and *O. profundus* KBZ 2-5 are gram-positive, motile, aerobic, rod-shaped
185 (0.2-0.4 μm and 0.5-0.6 μm respectively) and are classified as biosafety level 1 bacteria. The
186 genus *Oceanobacillus* has been previously isolated from wastewater (Nam et al., 2008), Korean
187 food (Whon et al., 2010), deep sea sediment core samples (Yu et al., 2014) and human gut (Lagier
188 et al., 2015). To the best of our knowledge, there are no reports indicating their potential
189 application in biotechnology, bioremediation or biosorption. Therefore, *O. profundus* KBZ 1-3

190 and *O. profundus* KBZ 2-5 isolated from Kabwe waste samples represent a novel *Oceanobacillus*
191 species that is being applied for the first time in a bioremediation study.

192

193 **3.2 Effect of Pb on microbial growth and urease activity of isolates**

194 Since the isolates are intended to be used in a heavily Pb-contaminated environment, the bacteria
195 were tested for the effect of Pb (II) in aqueous solution. Fig. 2 shows the effect of Pb on both
196 microbial growth and urease activity of *O. profundus* KBZ 1-3 and *O. profundus* KBZ 2-5. Both
197 bacteria displayed similar growth patterns, i.e., increased growth in lead-free media and a slight
198 growth retardation in the presence of 50 mg/L lead (Fig. 2). Therefore, the effects of lead on
199 microbial growth were minimal, likely because these bacteria were isolated from a lead-
200 contaminated site with bioavailable concentration of Pb (II) of 7.8 mg/L in leach plant residues
201 whereas kiln slag had 5.40 mg/L bioavailable lead concentration. The bioavailable fraction
202 determines the potential harm of a contaminant on the receptor (Ng et al., 2015). Similar results
203 have been reported from previous research where growth retardation was exhibited by a
204 halotolerant bacteria in the presence of lead isolated from an abandoned mine in South Korea
205 (Kang et al., 2015).

206 The effect of lead on urease activity was studied because it is crucial in MICP-mediated
207 bioremediation for the abandoned Kabwe mine site. As shown in Fig. 2, the urease activity *O.*
208 *profundus* KBZ 2-5 is higher than that of *O. profundus* KBZ 1-3; both bacteria expressed the
209 highest urease activity after 48 h incubation with only appreciable levels at 24 h and 72 h. Only
210 *O. profundus* KBZ 2-5 maintained the enzyme activity until 96 h. The urease activities of both
211 isolates were not significantly affected by lead, probably because they were isolated from a lead-
212 contaminated site. Higher urease activity is very important in MICP-mediated processes because
213 it has a significant impact on the rate of carbonate production that consequently precipitates out
214 as CaCO₃. The results clearly show increased growth and urease activity by *O. profundus* KBZ

215 1-3 and *O. profundus* KBZ 2-5 in the absence and presence of lead. Overall, both bacteria are
216 suitable for the biocementation of mine waste contaminated with Pb because they are Pb-tolerant,
217 with high growth and urease activities.

218

219 **3.3 Determination of the optimal Ca²⁺/urea concentration**

220 Calcium and urea are the two most important ingredients for carrying out the MICP process.
221 The urease enzyme produced from the bacteria hydrolyzes urea (CO(NH₂)₂) to ammonium
222 (NH₄⁺) and carbonate (CO₃²⁻), which leads to the precipitation of CaCO₃ in the presence of
223 calcium ions (Ca²⁺). Therefore, the tolerance to and the optimal concentrations of calcium and
224 urea may vary from one bacterial species to another, requiring the determination of optimal
225 conditions for *O. profundus* KBZ 1-3 and *O. profundus* KBZ 2-5. Fig. 3 shows the amount of
226 precipitate formed by both bacteria when the concentration ratio of calcium:urea = 1:1; equimolar
227 concentrations were used because they are more effective, according to a previous study (Soga
228 and Qabany, 2013). As shown in Fig. 3, increasing the equimolar calcium and urea concentrations
229 also increased the amount of precipitate. In this study, we used the equimolar concentration of
230 0.5 M for calcium and urea. Previous studies have indicated that a low equimolar concentration
231 in the solution should be used to ensure a uniform consistency of CaCO₃ precipitation (Mujah et
232 al., 2017). Since a solution with low concentration may produce a more uniform precipitation
233 pattern, even though higher concentrations produce higher amounts of CaCO₃ precipitate, a lower
234 concentration was selected. In this study, both *O. profundus* KBZ 1-3 and *O. profundus* KBZ 2-
235 5 precipitated spherical calcite crystals (Supplementary Fig. S4). Calcite is the preferred form of
236 CaCO₃ for biocementation because it is the most stable, compared to the other polymorphic forms
237 such as aragonite and vaterite (Boulos et al., 2014).

238 The two isolates precipitated CaCO₃, which can be used as an inert covering for mine
239 wastes. Capping is advantageous as a treatment technology because it is a permanent remedy that

240 can also eliminate dust, thus addressing chronic risks of Pb poisoning to humans and other
241 ecological receptors (Bellenfant et al., 2013; Johnson et al., 1992; Lottermoser, 2011).

242

243 **3.4 Strength, SEM and XRD analyses of solidified sand**

244 UCS was measured to characterize the strength of cemented sand. Fig. 4 shows the
245 appearance of the control and biocemented sand, while Table 1 shows the corresponding
246 estimated values of UCS at the top, middle, and bottom parts of the specimens.

247 The control specimen registered no strength while sand biocemented by *O. profundus*
248 KBZ 1-3 under immersed and flow-through conditions had maximum estimated UCS values of
249 3.2 MPa and 2.0 MPa, respectively. The strength of sand biocemented by *O. profundus* KBZ 2-
250 5 under immersed and flow-through conditions were 5.5 MPa and 3.5 MPa, respectively. Sand
251 biocemented by *O. profundus* KBZ 2-5 was stronger probably because of higher urease activity
252 (Fig. 2) and the greater amount of precipitate formed compared to *O. profundus* KBZ 1-3 (Fig.
253 3). Since the difference in UCS is marginal, both bacteria may be useful for solidification.
254 Additionally, both immersed and flow-through cementation methods provided more strength.
255 Therefore, both types of injection methods can be used for solidifying sand. The results imply
256 that the increased strength of biocemented sand has the potential to prevent the airborne transport
257 of metallic dust by prevailing winds and to reduce infiltration; these benefits are similar to those
258 of conventional cement, used worldwide for capping mining waste (Batchelor, 2006; Sobiecka,
259 2013).

260 To further confirm the role of MICP, biocemented samples were examined by SEM and
261 XRD. Fig. 5 shows typical SEM images and the corresponding XRD patterns of the control (a)
262 and biocemented sand (b, c). The control samples present a typical morphology of sand and
263 appear as discrete particles, while the biocemented samples show prominent crystalline deposits
264 on the surface and between sand particles. The SEM micrographs verify the effectiveness of the

265 so-called bridging phenomenon mediated by MICP, i.e. the deposited CaCO_3 forms bridges
266 between particles as part of the binding process (Mujah et al., 2017; Ng et al., 2012;
267 Rowshanbakht et al., 2016).

268 The XRD analysis reveals that the control specimens are composed of only quartz, while
269 the biocemented sand includes calcite. Calcite is formed due to the ureolysis and subsequent
270 precipitation of CaCO_3 . The XRD results allowed us to conclude that MICP plays an important
271 role in the solidification of sand.

272 The major pathway for Pb to gain entry into the blood of humans and animals around the Kabwe
273 mine site is through inhalation and injection of dust particles emanating from the abandoned mine
274 wastes dumps, since the prevailing winds blow mostly from east (the mine site) to west (toward
275 a large residential area) (Tembo et al., 2006; Yabe et al., 2011, 2013, 2015, 2018). Immobilizing
276 the sand via MICP aggregates the sandy material (Fig. 4), making it less susceptible to being
277 blown by wind. This significantly curtails the Pb exposure pathway to humans and animals in
278 and around the mine site. MICP using indigenous bacteria can be immediate and easily
279 implemented because all the required materials such as sand, indigenous bacteria, nutrients,
280 calcium source, and urea are locally available. Some researchers have proposed the use of
281 alternative locally available nutrients and calcium sources such as lactose mother liquor (Achal
282 et al., 2009) and eggshells (Choi et al., 2016), which also demonstrates the flexibility of the
283 process. In a similar way, locally available resources required for capping will be utilized
284 including the indigenous bacteria making the bioremediation process cheap, sustainable, and less
285 likely to change the integrity of the local biodiversity.

286

287 **3.5 CaCO_3 content of biocemented sand**

288 To elucidate the strength of the biocement, the CaCO_3 content precipitated between sand grains
289 of specimens was evaluated. Only the top parts of the control and biocemented sand were

290 evaluated. The control contained no CaCO_3 . On the other hand, sand biocemented by immersed
291 and flow methods using *O. profundus* KBZ 1-3 had 6.5 ± 0.10 % and 3.0 ± 0.20 % CaCO_3 ,
292 respectively, while sand biocemented by *O. profundus* KBZ 2-5 by immersed and flow methods
293 had 10.0 ± 0.20 % and 8.0 ± 0.20 % CaCO_3 , respectively. CaCO_3 content is one of the most
294 important engineering factors in MICP-mediated processes. Its relationship with UCS is shown
295 in Fig. 6. As seen in the results, the control contained no CaCO_3 and hence had no strength. The
296 UCS of biocemented sand increased with CaCO_3 content (indicated by the pink and green
297 circles), which suggests that CaCO_3 plays a significant role in the strength of sand, which has
298 also been elucidated by previous studies (Amarakoon and Kawasaki, 2018). Furthermore, more
299 precipitation of CaCO_3 occurred in immersed method probably due to accumulation of reactants
300 and bacteria when the syringe is closed. The findings are in agreement with results reported by
301 Keykha et al., (2019) when they solidified soil and maintained immersed conditions at all times
302 and achieved higher UCS. Similarly, Gomez et al., (2018) reported that with the largest calcite
303 contents were observed near the injection which had higher UCS when they conducted
304 biostimulation and concluded that reductions in calcite content from the top were due to solution
305 mixing and/or urea hydrolysis. In both treatment methods, the mid-top area has higher UCS
306 because the reactants first contact the mid-top when injected where they are spent, depleted and
307 less effective hence the lower UCS in middle and bottom area. The difference in UCS between
308 the treatment methods lies in the contact time of the reactants in the column. In the immersed
309 method, the reactants have more contact time during immersed compared to flow through method
310 where reactants flow through the column in a shorter time hence the higher UCS in the immersed
311 method compared to flow through method.

312

313 **3.6 Hydraulic conductivity**

314 Hydraulic conductivity is a measure of how easily water can pass through a material. During
315 immobilization, reduced hydraulic conductivity is desired because it reduces the ability of water

316 to contact contaminants, and, therefore, reduces contaminant leaching rates. Hydraulic
317 conductivity tests were performed on the sand before and after MICP treatment. Before treatment,
318 the hydraulic conductivity was 1.4×10^{-3} m/s. Biocemented sand treated by the immersed and
319 flow-through methods using *O. profundus* KBZ 1-3 reduced the water permeability of sand to
320 9.6×10^{-8} m/s and 2.4×10^{-7} m/s, respectively. Similarly, *O. profundus* KBZ 2-5 reduced the water
321 permeability of sand to 8.9×10^{-8} m/s and 2.5×10^{-7} m/s when treated by immersed and flow-
322 through methods, respectively. In all the cases, the hydraulic conductivity improved by more than
323 three orders of magnitude for both immersed and flow-through methods. The reduced hydraulic
324 conductivity achieved in this study has the potential to limit the entrance of water and oxygen
325 into the dump, and hence reduce the leaching of heavy metals. This reduction in permeability is
326 consistent with results of previous studies (Achal et al., 2013, Eryürük et al., 2015).

327 Other studies have proposed vegetation cover (Chehregani et al., 2009, Leteinturier et al.,
328 2001) and synthetic cover (Fourie et al., 2010; Mazzieri et al., 2013) to cap mine wastes.
329 Vegetation cover is desirable because like MICP, it reduces surface erosion and a large proportion
330 of percolating water is lost to the atmosphere through transpiration, reducing the concentrations
331 of soluble heavy metals entering watercourses. However, this method would be difficult to
332 implement in Kabwe, because vegetation growth is not possible at the site due to lack of nutrients
333 and high levels of toxic trace elements at the site (Leteinturier et al., 2001). On the other hand,
334 synthetic covers are uneconomical and expensive, especially compared to the MICP technique.
335 Due to its originality and sustainability, MICP has recently gained much attention from
336 researchers around the world as a replacement for conventional concrete (Seifan et al., 2016).
337 Conventional physicochemical methods have already been tested to clean the environment.
338 However, most of these methods are costly, perform sub-optimally, and produce secondary
339 sludge, making the cleanup process expensive and unsustainable, requiring large inputs of energy
340 and large quantities of chemical reagents (Jena and Dey, 2016).

341

342 **4 Conclusions**

343 The abandoned lead and zinc mine wastes in Kabwe mine continue to pose a serious threat to
344 the quality of human health, water, and soil. We have shown in this study that microbially induced
345 calcium carbonate precipitation (MICP) mediated by indigenous ureolytic bacteria
346 *Oceanobacillus profundus* KBZ 1-3 and KBZ 2-5 can be used to solidify sand, thus preventing
347 dust formation and water infiltration. Both bacteria were able to tolerate Pb and mediate the
348 formation of CaCO₃ bioprecipitates, which was confirmed to be calcite by XRD analysis. The
349 biocemented sand achieved maximum unconfined compressive strength values of 3.2 MPa and
350 5.5 MPa, which are useful enough to prevent Pb dust particles from being blown away by
351 prevailing winds and to prevent water erosion. Combined with reduced hydraulic conductivity of
352 9.6×10^{-8} m/s and 8.9×10^{-8} m/s mediated by *Oceanobacillus profundus* KBZ 1-3 and KBZ 2-5,
353 respectively, the process is expected to retard heavy metal leaching due to the lack of oxygen and
354 water resulting from reduced infiltration. In a future study, we intend to implement this
355 laboratory-proven procedure in-situ to determine the durability of biocemented materials under
356 field conditions.

357

358 **Declarations of interest: none**

359 **Appendix A. Supplementary material**

360

361 **Acknowledgments**

362 This work was partly supported by JST/JICA, SATREPS (Science and Technology Research
363 Partnership for Sustainable Development) and JSPS KAKENHI under grant numbers
364 JP18H03395 and JP16H04404.

365

366 **References**

- 367 Achal, V., Mukherjee, A., Basu, P.C., Reddy, M.S., 2009. Lactose mother liquor as an alternative
368 nutrient source for microbial concrete production by *Sporosarcina pasteurii*. J. Ind.
369 Microbiol. Biotechnol. 36, 433–438. doi:10.1007/s10295-008-0514-7
- 370 Achal, V., Pan, X., Lee, D.J., Kumari, D., Zhang, D., 2013. Remediation of Cr(VI) from
371 chromium slag by biocementation. Chemosphere 93, 1352–1358.
372 doi:10.1016/j.chemosphere.2013.08.008
- 373 Amarakoon, G.G.N.N., Kawasaki, S., 2018. Factors affecting sand solidification using MICP
374 with *Pararhodobacter* sp. Mater. Trans. 59, 72–81. doi:10.2320/matertrans.M-M2017849
- 375 Batchelor, B., 2006. Overview of waste stabilization with cement. Waste Manag. 26, 689–698.
376 doi:10.1016/j.wasman.2006.01.020
- 377 Bellenfant, G., Guezennec, Anne-Gwenaëlle Bodénan, F., D’Hugues, P., Cassard, D., 2013.
378 Reprocessing of mining waste: Combining environmental management and metal recovery?
379 Mine Clos. 571–582.
- 380 BMR Group PLC, 2019. Tailings stockpiles [WWW Document]. URL
381 http://www.bmrplc.com/tailings_stockpiles.php (accessed 1.25.19).
- 382 Boulos, R.A., Zhang, F., Tjandra, E.S., Martin, A.D., Spagnoli, D., Raston, C.L., 2014. Spinning
383 up the polymorphs of calcium carbonate. Sci. Rep. 4, 1–6. doi:10.1038/srep03616
- 384 Chehregani, A., Noori, M., Yazdi, H.L., 2009. Phytoremediation of heavy-metal-polluted soils:
385 Screening for new accumulator plants in Angouran mine (Iran) and evaluation of removal
386 ability. Ecotoxicol. Environ. Saf. 72, 1349–1353. doi:10.1016/j.ecoenv.2009.02.012
- 387 Chen, X., Guo, H., Cheng, X., 2017. Heavy metal immobilisation and particle cementation of
388 tailings by biomineralisation. Environ. Geotech. 1–7. doi:10.1680/jenge.15.00068
- 389 Choi, S., Wu, S., Chu, J., 2016. Biocementation for sand using an eggshell as calcium source. J.
390 Geotech. Geoenvironmental Eng. 142, 2–5. doi:10.1061/(ASCE)GT.1943-5606.0001534.

391 Danjo, T., Kawasaki, S., 2015. Artificial beachrock formation through sand solidification towards
392 the inhibit of coastal erosion. *Int. J. GEOMATE* 9, 1528–1533.

393 Eryürük, K., Yang, S., Suzuki, D., Sakaguchi, I., Akatsuka, T., Tsuchiya, T., Katayama, A., 2015.
394 Reducing hydraulic conductivity of porous media using CaCO₃ precipitation induced by
395 *Sporosarcina pasteurii*. *J. Biosci. Bioeng.* 119, 331–336. doi:10.1016/j.jbiosc.2014.08.009

396 Fourie, A.B., Bouazza, A., Lupo, J., 2010. Improving the performance of mining infrastructure
397 through the judicious use of geosynthetics. 9th Int. Conf. Geosynth. Brazil.

398 Gomez, M.G., Graddy, C.M.R., DeJong, J.T., Nelson, D.C., Tsesarsky, M., 2018. Stimulation of
399 native microorganisms for biocementation in samples recovered from field scale treatment
400 depths. *J. Geotech. Geoenvironmental Eng.* 144, 1–13. doi:10.1061/(ASCE)GT.1943-
401 5606.0001804.

402 Hukue, M., Kato, Y., Nakamura, T., Moriyama, N., 2001. A method for determining carbonate
403 content for soils and evaluation of the results. *Japanese Geotech. Soc.* 49, 2669. *In Japanese*

404 Jena, S., Dey, S.K., 2016. Heavy Metals. *Am. J. Environ. Stud.* 1, 48–60.

405 Johnson, M.S., Cooke, J.A., Stevenson, J.K.W., 1992. Revegetation of metalliferous wastes and
406 and after metal mining, *Mining and its Environmental Impact*.

407 Kang, C.H., Oh, S.J., Shin, Y., Han, S.H., Nam, I.H., So, J.S., 2015. Bioremediation of lead by
408 ureolytic bacteria isolated from soil at abandoned metal mines in South Korea. *Ecol. Eng.*
409 74, 402–407. doi:10.1016/j.ecoleng.2014.10.009

410 Keykha, H.A., Mohamadzadeh, H., Asadi, A., Kawasaki, S., 2019. Ammonium-free carbonate-
411 producing bacteria as an ecofriendly soil biostabilizer. *Geotech. Test. J.* 42, 20170353.
412 doi:10.1520/GTJ20170353

413 Khan, M.N.H., Amarakoon, G.G.N.N., Shimazaki, S., Kawasaki, S., 2015. Coral sand
414 solidification test based on microbially induced carbonate precipitation using ureolytic
415 bacteria. *Mater. Trans.* 56, 1725–1732. doi:10.2320/matertrans.M-M2015820

416 Kim, J.H., Lee, J.Y., 2018. An optimum condition of MICP indigenous bacteria with
417 contaminated wastes of heavy metal. *J. Mater. Cycles Waste Manag.* 1–9.
418 doi:10.1007/s10163-018-0779-5

419 Kosnett, M.J., Wedeen, R.P., Rothenberg, S.J., Hipkins, K.L., Materna, B.L., Schwartz, B.S., Hu,
420 H., Woolf, A., 2007. Recommendations for medical management of adult lead exposure.
421 *Environ. Health Perspect.* 115, 463–471. doi:10.1289/ehp.9784

422 Kribek, B., Nyambe, I.A., Njamu, F., Chitwa, G., Ziwa, G., 2009. Assessment of impacts of
423 mining and mineral processing on the environment and human health in selected regions of
424 the Central and Copperbelt Provinces of Zambia. Report No. RP/3/2008 for years 2008-
425 2010. Lusaka.

426 Lagier, J.C., Khelaifia, S., Azhar, E.I., Croce, O., Bibi, F., Jiman-Fatani, A.A., Yasir, M., Helaby,
427 H. Ben, Robert, C., Fournier, P.E., Raoult, D., 2015. Genome sequence of *Oceanobacillus*
428 *picturae* strain S1, an halophilic bacterium first isolated in human gut. *Stand. Genomic Sci.*
429 10, 1–9. doi:10.1186/s40793-015-0081-2

430 Leteinturier, B., Laroche, J., Matera, J., Malaisse., F., 2001. Reclamation of lead/zinc processing
431 wastes at Kabwe, Zambia: a phytogeochemical approach. *South Africa J. Sci.* 97, 624–627.

432 Lottermoser, B.G., 2011. Recycling, reuse and rehabilitation of mine wastes. *Elements* 7, 405–
433 410. doi:10.2113/gselements.7.6.405

434 Mazzieri, F., Di Emidio, G., Fratolocchi, E., Di Sante, M., Pasqualini, E., 2013. Permeation of
435 two GCLs with an acidic metal-rich synthetic leachate. *Geotext. Geomembranes* 40, 1–11.
436 doi:10.1016/j.geotexmem.2013.07.011

437 Mufinda, B., 2015. A History of Mining in Broken Hill (Kabwe): 1902-1929. University of the
438 Free State.

439 Mujah, D., Shahin, M.A., Cheng, L., 2017. State-of-the-art review of biocementation by
440 microbially induced calcite precipitation (MICP) for soil stabilization. *Geomicrobiol. J.* 34,

441 524–537. doi:10.1080/01490451.2016.1225866

442 Mwandira, W., Nakashima, K., Kawasaki, S., 2017. Bioremediation of lead-contaminated mine
443 waste by *Pararhodobacter* sp. based on the microbially induced calcium carbonate
444 precipitation technique and its effects on strength of coarse and fine grained sand. *Ecol. Eng.*
445 109, 57–64. doi:10.1016/j.ecoleng.2017.09.011

446 Nam, I.H., Roh, S.B., Park, M.J., Chon, C.M., Kim, J.G., Jeong, S.W., Song, H., Yoon, M.H.,
447 2016. Immobilization of heavy metal contaminated mine wastes using *Canavalia ensiformis*
448 extract. *Catena* 136, 53–58. doi:10.1016/j.catena.2015.07.019

449 Nam, J.H., Bae, W., Lee, D.H., 2008. *Oceanobacillus caeni* sp. nov., isolated from a Bacillus-
450 dominated wastewater treatment system in Korea. *Int. J. Syst. Evol. Microbiol.* 58, 1109–
451 1113. doi:10.1099/ijs.0.65335-0

452 Ng, J.C., Juhasz, A., Smith, E., Naidu, R., 2015. Assessing the bioavailability and bioaccessibility
453 of metals and metalloids. *Environ. Sci. Pollut. Res.* 22, 8802–8825. doi:10.1007/s11356-
454 013-1820-9

455 Ng, W., Lee, M., Hii, S., 2012. An overview of the factors affecting microbial-induced calcite
456 precipitation and its potential application in soil improvement. *World Acad. Sci. Eng.*
457 *Technol.* 62, 723–729.

458 Rowshanbakht, K., Khomehchiyan, M., Sajedi, R.H., Nikudel, M.R., 2016. Effect of injected
459 bacterial suspension volume and relative density on carbonate precipitation resulting from
460 microbial treatment. *Ecol. Eng.* 89, 49–55. doi:10.1016/j.ecoleng.2016.01.010

461 Salifu, E., MacLachlan, E., Iyer, K.R., Knapp, C.W., Tarantino, A., 2016. Application of
462 microbially induced calcite precipitation in erosion mitigation and stabilisation of sandy soil
463 foreshore slopes: A preliminary investigation. *Eng. Geol.* 201, 96–105.
464 doi:10.1016/j.enggeo.2015.12.027

465 Seifan, M., Samani, A.K., Berenjian, A., 2016. Bioconcrete: next generation of self-healing

466 concrete. *Appl. Microbiol. Biotechnol.* 100, 2591–2602. doi:10.1007/s00253-016-7316-z

467 Sobiecka, E., 2013. Investigating the chemical stabilization of hazardous waste material (fly ash)

468 encapsulated in Portland cement. *Int. J. Environ. Sci. Technol.* 10, 1219–1224.

469 doi:10.1007/s13762-012-0172-1

470 Soga, A.A., Qabany, K., 2013. Effect of chemical treatment used in MICP on engineering

471 properties of cemented soils. *Géotechnique* Volume 63, 331–339.

472 Tembo, B.D., Sichilongo, K., Cernak, J., 2006. Distribution of copper, lead, cadmium and zinc

473 concentrations in soils around Kabwe town in Zambia. *Chemosphere* 63, 497–501.

474 doi:10.1016/j.chemosphere.2005.08.002

475 Torres-Aravena, Á., Duarte-Nass, C., Azócar, L., Mella-Herrera, R., Rivas, M., Jeison, D., 2018.

476 Can microbially induced calcite precipitation (MICP) through a uelytic pathway be

477 successfully applied for removing heavy metals from wastewaters? *Crystals* 8, 438.

478 doi:10.3390/cryst8110438

479 Whon, T.W., Jung, M.-J., Roh, S.W., Nam, Y.-D., Park, E.-J., Shin, K.-S., Bae, J.-W., 2010.

480 *Oceanobacillus kimchii* sp nov Isolated from a Traditional Korean Fermented Food. *J.*

481 *Microbiol.* 48, 862–866. doi:10.1007/s12275-010-0214-7

482 Wiktor, V., Jonkers, H.M., 2011. Quantification of crack-healing in novel bacteria-based self-

483 healing concrete. *Cem. Concr. Compos.* 33, 763–770.

484 doi:10.1016/j.cemconcomp.2011.03.012

485 Yabe, J., Nakayama, S.M.M., Ikenaka, Y., Muzandu, K., Choongo, K., Mainda, G., Kabeta, M.,

486 Ishizuka, M., Umemura, T., 2013. Metal distribution in tissues of free-range chickens near

487 a lead-zinc mine in Kabwe, Zambia. *Environ. Toxicol. Chem.* 32, 189–192.

488 doi:10.1002/etc.2029

489 Yabe, J., Nakayama, S.M.M., Ikenaka, Y., Muzandu, K., Ishizuka, M., Umemura, T., 2011.

490 Uptake of lead, cadmium, and other metals in the liver and kidneys of cattle near a lead-zinc

491 mine in Kabwe, Zambia. Environ. Toxicol. Chem. 30, 1892–1897. doi:10.1002/etc.580

492 Yabe, J., Nakayama, S.M.M., Ikenaka, Y., Yohannes, Y.B., Bortey-Sam, N., Kabalo, A.N.,

493 Ntapisha, J., Mizukawa, H., Umemura, T., Ishizuka, M., 2018. Lead and cadmium excretion

494 in feces and urine of children from polluted townships near a lead-zinc mine in Kabwe,

495 Zambia. Chemosphere 202, 48–55. doi:10.1016/j.chemosphere.2018.03.079

496 Yabe, J., Nakayama, S.M.M., Ikenaka, Y., Yohannes, Y.B., Bortey-Sam, N., Oroszlany, B.,

497 Muzandu, K., Choongo, K., Kabalo, A.N., Ntapisha, J., Mweene, A., Umemura, T.,

498 Ishizuka, M., 2015. Lead poisoning in children from townships in the vicinity of a lead-zinc

499 mine in Kabwe, Zambia. Chemosphere 119, 941–947.

500 doi:10.1016/j.chemosphere.2014.09.028

501 Yu, C., Yu, S., Zhang, Z., Li, Z., Zhang, X.H., 2014. *Oceanobacillus pacificus* sp. nov., isolated

502 from a deep-sea sediment. Int. J. Syst. Evol. Microbiol. 64, 1278–1283.

503 doi:10.1099/ijs.0.056481-0

504 Zhu, X., Li, W., Zhan, L., Huang, M., Zhang, Q., Achal, V., 2016. The large-scale process of

505 microbial carbonate precipitation for nickel remediation from an industrial soil. Environ.

506 Pollut. 219, 149–155. doi:10.1016/j.envpol.2016.10.047

507

508 **Fig. 1.** (a) Location of soil sampling sites and the different mine wastes at the abandoned mine,

509 Kabwe, Zambia (b) Appearance of leach plant residues and kiln slag.

510 **Fig. 2.** Microbial growth and urease activity of (a) *O. profundus* KBZ 1-3, and (b) *O. profundus*

511 KBZ 2-5. Error bars indicate standard deviations of three independent replicates. (U=μmol urea

512 hydrolyzed/min)

513 **Fig. 3.** Weight of CaCO₃ bioprecipitated by *O. profundus* KBZ 1-3 and *O. profundus* KBZ 2-5

514 at different equimolar concentrations of calcium and urea. Error bars indicate the standard

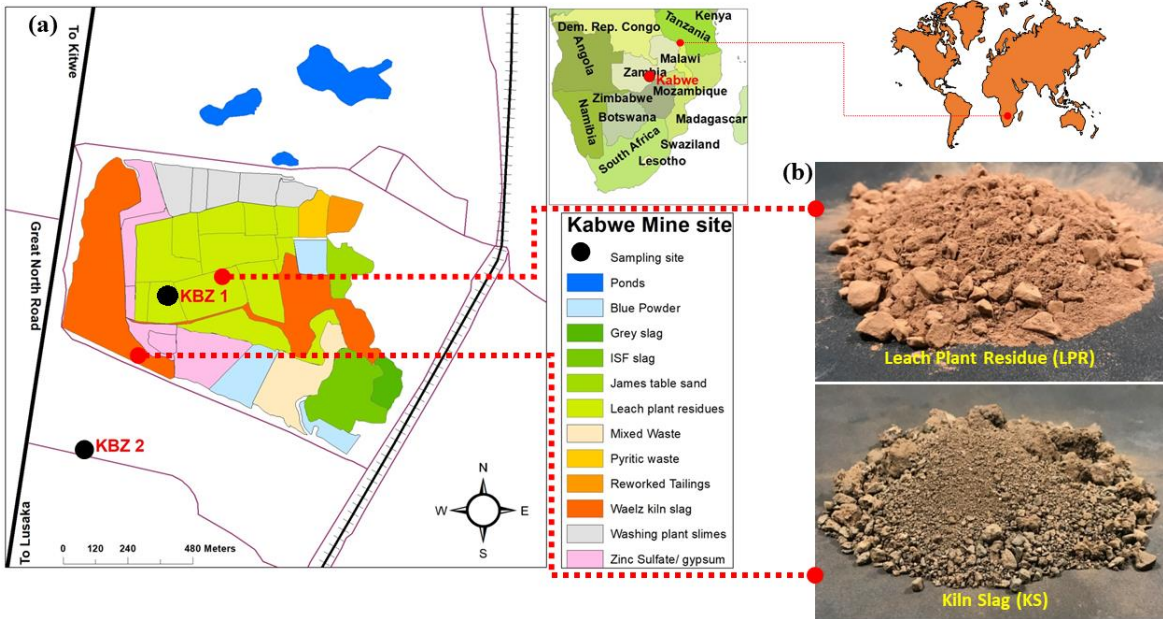
515 deviation of three independent replicates.

516 **Fig. 4.** Comparative view of control and biocemented sand **obtained** by the immersed and flow-
517 through methods facilitated by *O. profundus* KBZ 1-3 and *O. profundus* KBZ 2-5.

518 **Fig. 5.** SEM view and the corresponding XRD analysis comparing (a) control specimen, (b)
519 biocemented sand prepared by the flow-through method using *O. profundus* KBZ 1-3, and (c)
520 biocemented sand prepared by the flow-through method using *O. profundus* KBZ 2-5.

521 **Fig. 6.** Relationship between UCS and CaCO₃ content of sand biocemented by *O. profundus* KBZ
522 1-3 and *O. profundus* KBZ 2-5

523



524
525
526

Fig. 7.

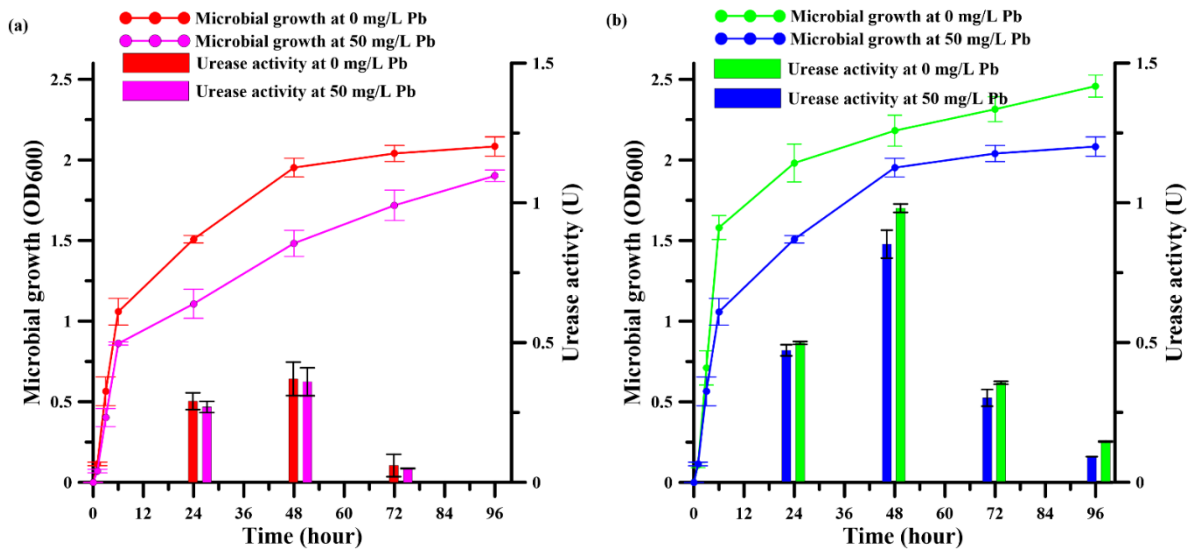


Fig. 8.

527
528
529

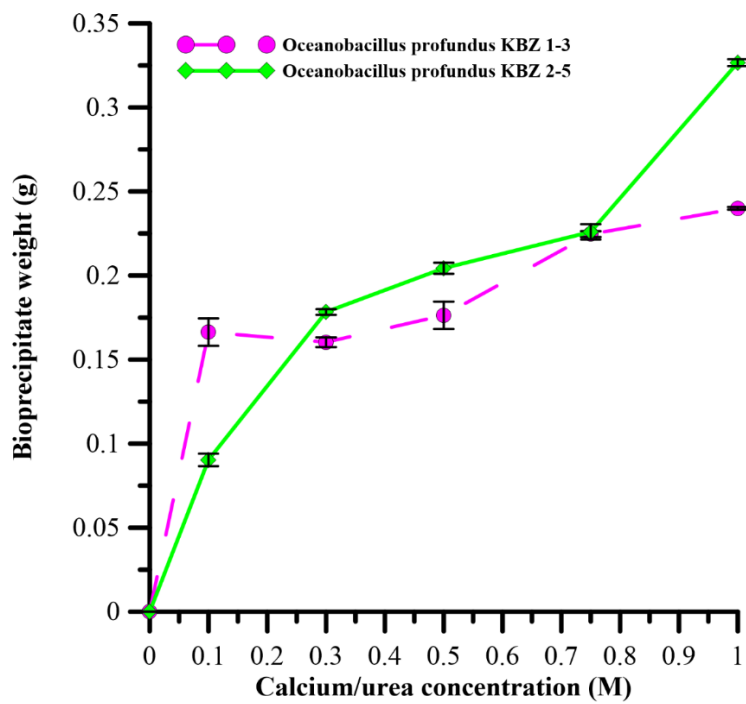


Fig. 9.

530

531

532

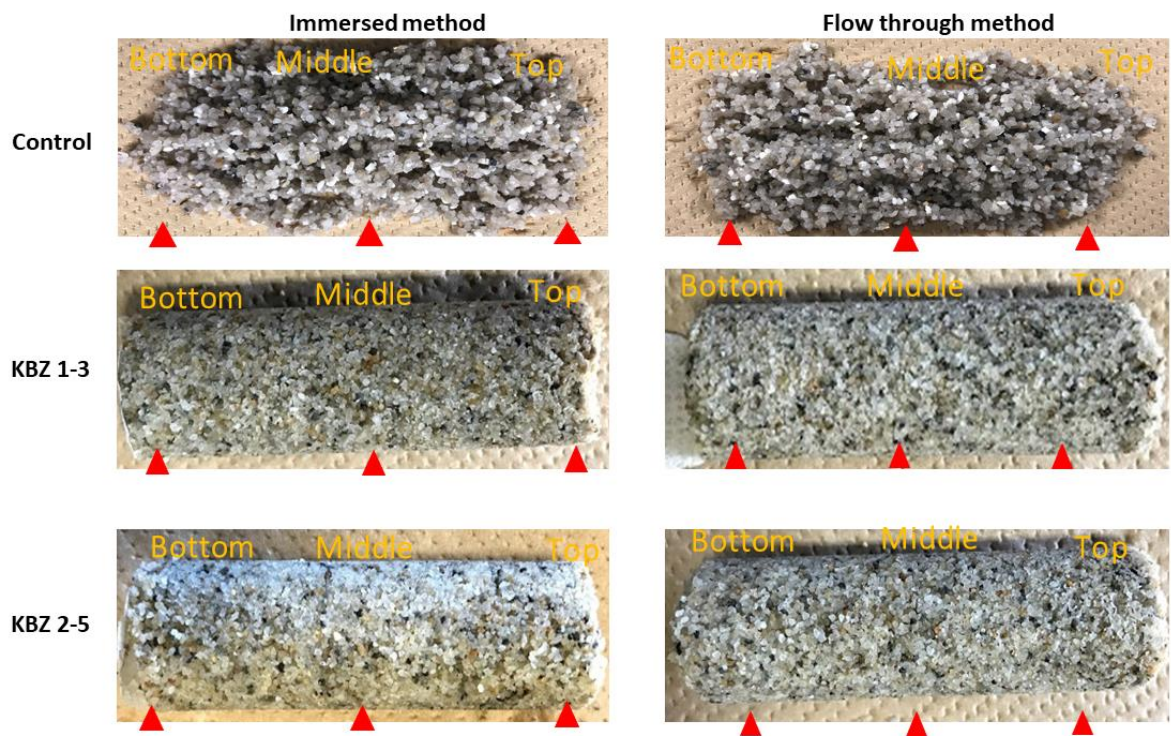


Fig. 10.

533

534

535

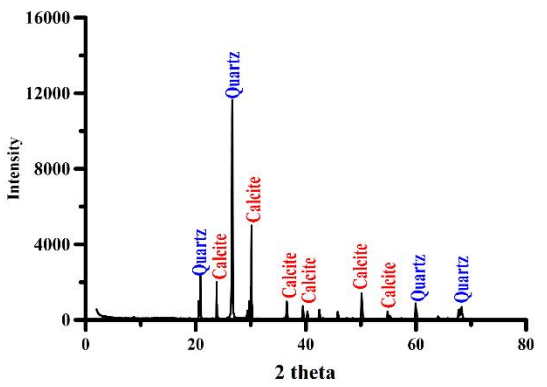
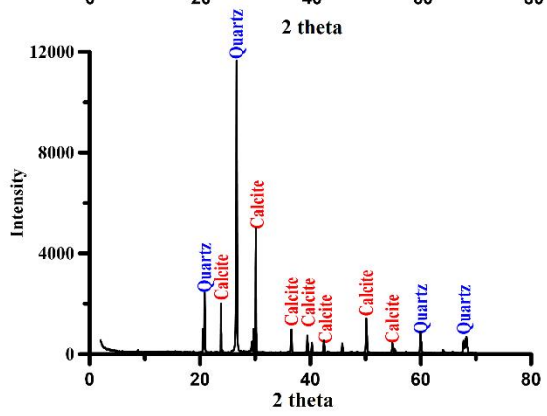
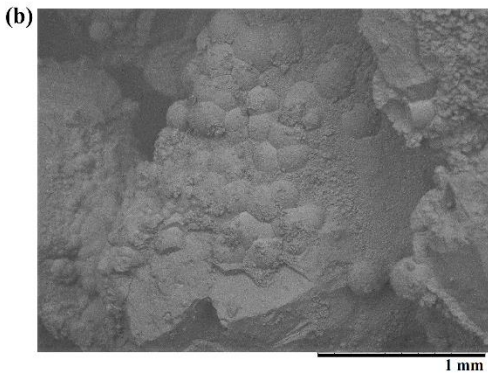
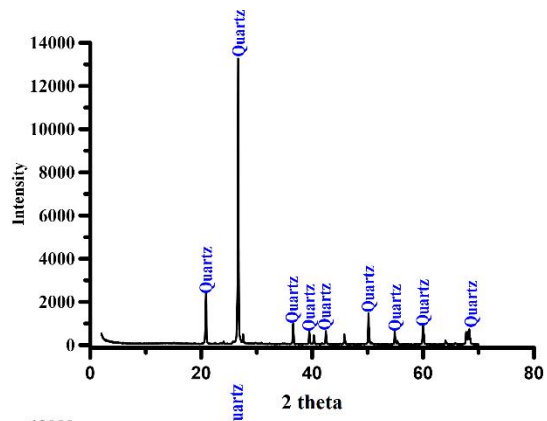
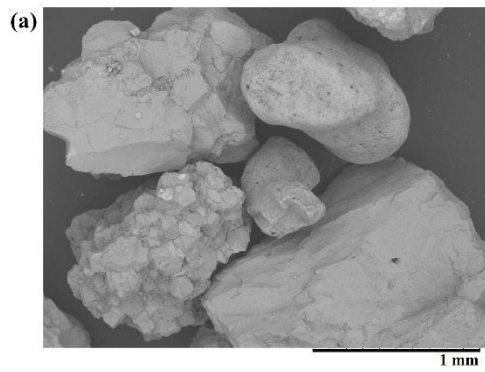


Fig. 11.

536

537

538

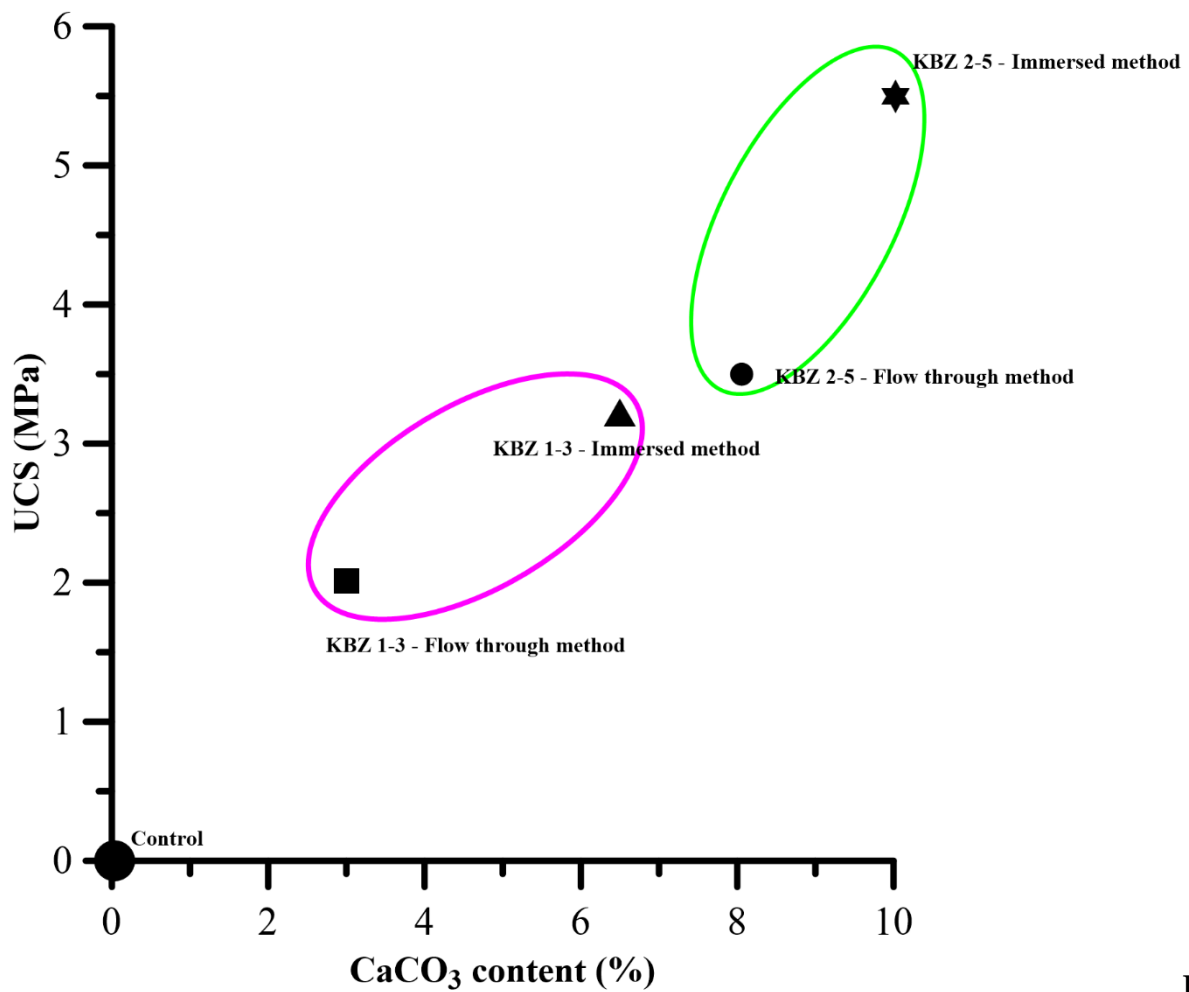


Fig.

12.

539
540
541

542 **Table 1.** Estimated UCS values of control and biocemented sand prepared by immersed and flow
543 through methods and mediated by *O. profundus* KBZ 1-3 and *O. profundus* KBZ 2-5

Specimen	Immersed method			Flow through method		
	Top	Middle	Bottom	Top	Middle	Bottom
Control	0	0	0	0	0	0
KBZ 1-3	3.2	1.8	1.4	2.0	1.4	1.0
KBZ 2-5	5.5	3.0	1.8	3.5	2.0	1.0

544
545

546 **Author contribution statement**

547 Wilson Mwandira (W.M.), Kazunori Nakashima (K.N.), Saturo Kawasaki (S.K.), Mayumi Ito
548 (M.I.), Tsutomu Sato (T.S.), Toshifumi Igarashi (T.I.), Meki Chirwa (M.C.), Kawawa Banda
549 (K.B.), Imasiku Nyambe (I.N.), Hokuto Nakata (H.N) Shouta Nakayama (S.N.), and Mayumi
550 Ishizuka (MA.I).

551

552 K.N., S.K., M.I., T.S., H.N, T.I., I.N., S.N., MA.I. designed, directed the project and were
553 responsible for funding acquisition. W.M., K.N., and S.K. conceived, planned and carried out the
554 experiments. W.M., M.C., H.N, M.I., T.S., and K.B. contributed to sample preparation. W.M.
555 K.N., S.K., T.S., T.I., and K.B. contributed to the interpretation of the results. W.M. took the lead
556 in writing the manuscript in consultation with K.N. and S.K. All authors provided critical
557 feedback and helped shape the research, analysis and manuscript.

558